Plant loading uncertainties and their incorporation in probabilistic creep damage assessments

N A Zentuti, J D Booker, R A W Bradford, C E Truman

Solid Mechanics Research Group, University of Bristol
Queens Building, University Walk, Bristol, BS8 1TR, United Kingdom

Abstract

This work presents methodologies for the examination of uncertainties in loading conditions for incorporation in probabilistic creep-fatigue (CF) crack initiation assessments. These approaches are based on the use of plant data for transient (TR) as well as steady-operating (SO) conditions, with both potentially having large contributions towards creep-fatigue damage. Conventionally, the stress-states in a boiler plant component are found using thermal and mechanical (elastic) finite element (FE) models. The main inputs to these models are the boiler steam temperatures, and the outputs are the six stress components (SCs) and the metal temperature (MT) at the assessment location(s) of interest. The proposed methodologies were developed based on experience gained from examining a tube-plate (TP) plant component, for which historical data was available. In a probabilistic assessment, the aim of these approaches is to replace time intensive FE runs with probabilistic alternatives which incorporate the variabilities in the loading conditions of interest. The value of these approaches lies in the avoidance of running FE models for every probabilistic trial (of which there typically may be more than 10^4*), which would be computationally prohibitive.*

Keywords: Creep, damage, plant loading, uncertainties, probabilistic

*Corresponding author
Email address: nz9512@bristol.ac.uk (N A Zentuti)

1. INTRODUCTION

An important part of assessing the lifetime of a plant component operating at high temperatures is predicting the amount of creep-fatigue (CF) damage that will have been accumulated by the end of service. Various codes and procedures provide guidance for estimating such damage, an example of which is the R5 procedure developed by EDF Energy [1, 2]. These assessment procedures are predominantly conservative, and therefore commonly use bounding values (deterministic) for material properties and loading conditions (temperatures and stresses). However, various uncertainties exist when assessing a plant component and incorporating a wide array of probabilistic techniques provides a systematic approach for addressing these uncertainties. These aim to provide a systematic understanding of the various uncertainties involved, which is not formally addressed by conventional deterministic assessments. As a result, and as part of a wider probabilistic framework, the ultimate interest is in the full utilisation of the available data for the purposes of quantifying the uncertainties which are simplified in deterministic approaches [3].

Plant loading conditions can be broadly considered to be either transient (TR) or steady-operation (SO). Both conditions can have large contributions to the CF damage. This work has been conducted with the R5 Volume 2/3 [1, 2] procedure in mind. However, the presented methodologies are flexible and can be implemented within other structural integrity applications. Two approaches are presented for probabilistically treating TR and SO conditions experienced by boiler plant components. The aim is to replace bounding stresses and temperatures with stochastic equivalents which are informed by plant measurements. The work is only concerned with the probabilistic treatment of elastic stresses, as these can be later translated to their elastic-plastic equivalents through a Neuber approximation which is inherent within the R5 Volume 2/3 procedure. The presented methodologies are contextualised through a case-study examining a plant component which has been used to prove their utility. This component

is a tubeplate (TP) for which relevant plant measurements were available. Finite element (FE) representations showing the geometry of the TP are shown in Figure 1. The probabilistic treatment of stresses and temperatures is part of an overarching probabilistic methodology for creep-fatigue initiation which is being explored in conjunction with the new probabilistic appendix (Appendix A15) to the R5 Volume 2/3 procedure.

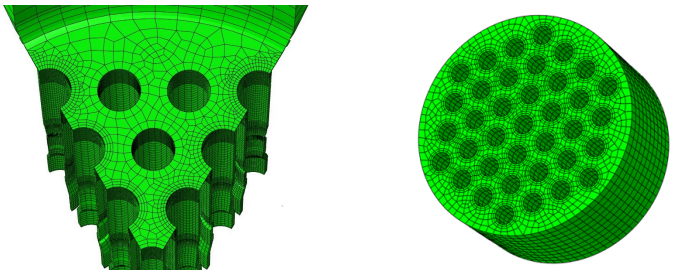

(a) One-sixth model (b) Full model.

Figure 1: Finite element geometries used for thermal and mechanical modelling of (a) transient and (b) steady-operation events.

2. METHODOLOGIES

2.1. TRANSIENT LOADING

Transients form a key part of constructing idealised hysteresis cycles (Figure 2); specifically constructing the extremities of these cycles which directly influence fatigue damage via the total cycle stress and strain ranges, and assessing the creep damage through the process of calculating the start-of-dwell stress (σ_B). To evaluate the stress range between the cycle extremities, all six stress components (SCs) at the *hot* and *cold* ends are required. All SCs are needed because the R5 Volume 2/3 procedure requires that Von Mises stress ranges are calculated from the ranges of individual SCs. Typically, the stress states for these extremities are obtained from transient thermal and mechanical (elastic) FE models. The key inputs for these analyses are the steam temperatures, while the outputs are the six SCs and metal temperatures at a predefined assessment

location. If a conventional deterministic assessment is being conducted, the most severe conditions for either extremities would be used. However, with the variabilities in transient conditions across the lifetime of a component, assuming fixed conditions for all TR events (typically based on severe and rare events) can introduce substantial conservatism.

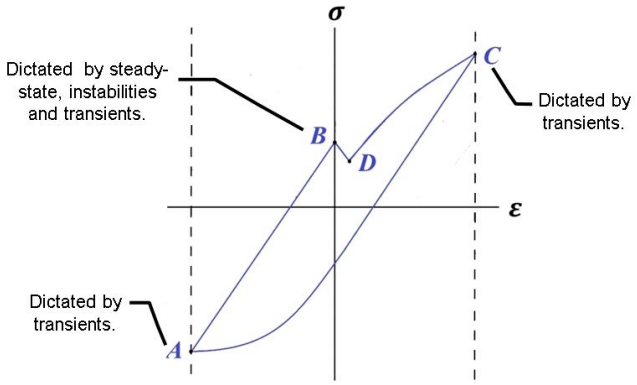

Figure 2: Schematic of a typical stress-strain (σ-ε) hysteresis cycle for a point located on the surface of a tubehole going through a reactor-trip to start-up (RT-SU) cycle.

This section presents an approach for the characterisation of variabilities in TR conditions by examining numerous events of the same type. Two types of transient events were considered in this work: start-up (SU) and reactor-trip (RT) events, which are characterised by rapid increases and decreases of loading temperatures respectively. A procedure was followed to treat these events which starts with the processing of raw plant data related to a component of interest. Concerning a CF damage assessment, a single transient event must be characterised by a single stress state (i.e. six SCs) and a characteristic metal temperature (MT). For a single transient event, and with the plant data as the starting point, the process for inferring the desired transient conditions is summarised in Figure 3.

The overall elastic stress range for the creep-fatigue cycle ($\Delta\sigma_{el}^{CA}$ in Figure

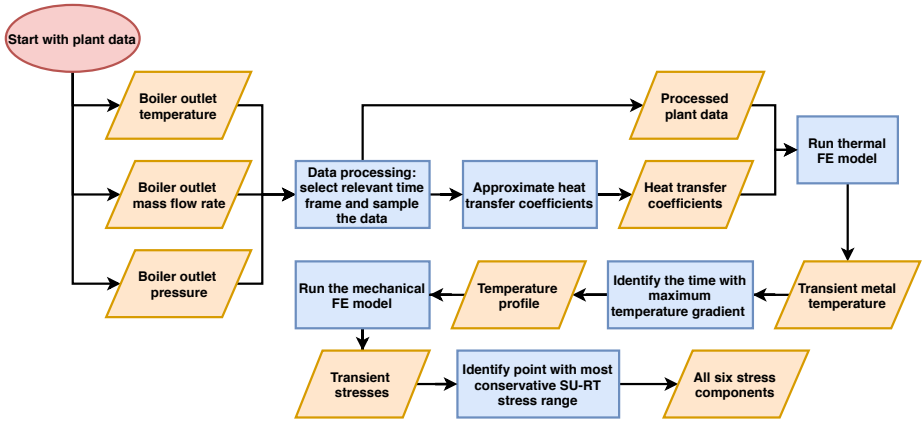

Figure 3: Flowchart showing the various stages involved in identifying the characteristic (peak) stress state during a single transient event. Points A and C are associated with SU and RT transients respectively.

2) is calculated based on the stress ranges of individual stress components:

$$\Delta\sigma_{el}^{CA} = \sigma_{el}^{RT} - \sigma_{el}^{SU} \tag{1}$$

where σ_{el}^{RT} and σ_{el}^{SU} represent the stress states at reactor-trip and start-up transients for a single cycle respectively. Although the notation suggests as much, this must not be interpreted as the algebraic difference between the peak Von Mises stresses for SU and RT. It must rather be understood as the Von Mises stress range formed from the component ranges between SU and RT. In the R5 procedure, $\Delta\sigma_{el}^{CA}$ has a direct effect on the total damage. However, due to the procedure for constructing the hysteresis cycle, this stress range affects creep and fatigue damages in different ways. To examine the effect of the magnitude of $\Delta\sigma_{el}^{CA}$ induced by the SU and RT transients, a deterministic assessment of the TP was used as a test case. For this purpose, a typical (fixed) stress state in steady-operation was assumed to evaluate point B shown in Figure 2. Figure 4 shows the effect of varying the magnitude of one transient type (say the SU) whilst keeping the other transient fixed. The key two conclusions that can be drawn are:

1. The most severe SU transient (i.e. producing the largest creep-fatigue

damage) is associated with the stress state that would produce the largest $\Delta\sigma_{el}^{CA}$, and is characterised by the largest (negatively signed) stress component.

2. The most severe RT transient is associated with the stress state that would produce the smallest $\Delta\sigma_{el}^{CA}$, and is characterised by the smallest (positively signed) stress components.

However, it must be noted that the above conclusions are strictly applicable when creep dominates over fatigue damage, which is the case for the TP. Furthermore, these are direct manifestations of the *symmetrisation* rule in the R5 Vol 2/3 procedure.

Figure 4 also indicates that the damage results are more sensitive to the variability in the SU stress state than its RT equivalent. Furthermore, a more compressive SU stress state results in higher damage which is in line with known experience; as a more compressive SU would imply a higher start of creep dwell (σ_B) stress. Therefore, for a single transient event, the characteristic stress-state and metal temperature for SU transients are taken at the location of most compressive SU stress component, which in this case defines the assessment location of interest. For this application, it was judged appropriate to obtain the desired quantities for the RT events at the same nodal location as the SU transients. Finally, the six SCs and MT were then examined to assess their variabilities by producing histograms for each quantity. Important correlations to be examined are the correlations between the SCs and the MT. For a single assessment location and for a single transient type, these can be described by a correlation matrix (sized 7×7) linking all characteristic loading quantities. Moreover, it is deemed important to explicitly consider any possible correlations between the stresses and temperatures. If these correlations are not taken into account, non-conservative effects maybe introduced, for example the high-stress and low-temperature combinations for SU could potentially produce larger damages. The Spearman (rank order) correlation coefficient was judged to be

appropriate for this application because it does not impose any restrictions on the type of distributions followed by the correlated parameters [4]. This makes the it viable for the application at hand which looks at discrete data. The topics of calculation and incorporation of the Spearman correlation are discussed in [5, 6, 7, 8].

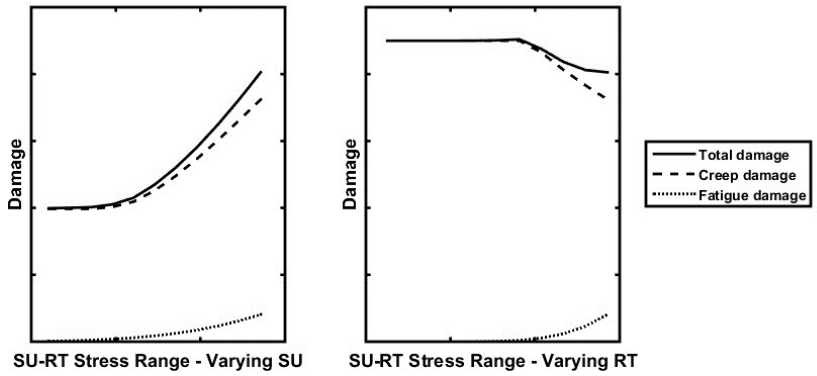

Figure 4: The effect of varying transient stress magnitudes on total, creep and fatigue damages obtained using a R5 Vol 2/3 deterministic assessment of the tubeplate. The x-axis on the left plot is increasing magnitude of *compressive* SU stress, whilst the one on the right plot is increasing magnitude of *tensile* RT stress.

2.2. STEADY-OPERATION LOADING

When assessing a plant component for CF damage, a key requirement is the approximation of the stresses during nominal operation (i.e. periods of power production). Due to variabilities in the plant operating temperatures, the stress state that a component might experience is ever-changing. As a result, the common practice of assuming a fixed (bounding) stress state which persists during long periods of the component's life can be overly conservative. In general, stress states are modelled using thermal and mechanical (elastic) FE models which can be computationally intensive, and therefore pose a limitation on their use in probabilistic calculations. This issue is explored in [9, 10] and the adoption of the Response Surface Method (RSM, which is effectively a multivariate regression approach [11, 12, 9]) was suggested for reducing compu-

tational efforts. This section presents a methodology for the use of plant data for inferring SO loading uncertainties. The purpose is to provide a systematic approach for constructing statistical, predictive models. These aim to act as surrogates to replace computationally intensive FE models in probabilistic assessments. They also attempt to predict the evolution of the stress state (an uncertain output) as a function of plant operating conditions (e.g. the steam temperatures).

Plant data process

For a plant component, the available SO plant data may be in the form of thermocouple (TC) measurements recorded during the component history. This history can be discretised into loading cycles, which in turn can be comprised of distinct events which represent various SO regimes between start-up and trip which define one cycle. Therefore, the raw plant data can be condensed into a single array comprising of event durations and the steam temperatures. For a single event, it was assumed that mean conditions (steam temperatures) persist for the duration of the event. In this work this new dataset will be referred to as the *processed history data*. A more detailed account of this process can be found in [5]. It must be emphasised that this arrangement of the raw history data does not necessarily influence the following stages of the proposed general approach. Thereafter, a batch of history events can be run in FE models, which produce temperature profiles for each event.

Assessment locations

For the SO stress analysis choosing an assessment point (i.e. point of most probable crack initiation) was required. Strictly speaking, and for creep dominated cases, the most likely point to initiate a crack first is the point (or node) which has a historic stress state which most frequently leads to the highest start-of-dwell stress, σ_B (point B in Figure 2). This requires that the transient stresses on either ends of the cycles, as well as the stress state during steady-operation

are considered. Identifying the point of maximum σ_B can be non-trivial especially when the variabilities of SU and RT transients are considered. However, the point of highest σ_B invariably corresponds to the highest stress range leading up to the creep dwell:

$$\Delta\sigma_{el}^{AB} = \sigma_{el}^{SO} - \sigma_{el}^{SU} \tag{2}$$

where σ_{el}^{SU} and σ_{el}^{SO} represent the elastic stress states for a SU transient and a SO condition respectively. Therefore, to simplify this analysis, the assessment point(s) are chosen as the node(s) which had the highest probability of producing the largest $\Delta\sigma_{el}^{AB}$ relative to all possible SU events. This process for identifying key assessment locations is described as follows:

1. For a single SO (static) FE run which represents an event, $\Delta\sigma_{el}^{AB}$ is calculated for all nodes. For this step all possible SU transients are considered in turn.
2. For each of the possibilities, record the node which had the highest stress range.
3. Repeat the procedure for all of the SO events considered.
4. For all SO events considered and for all SU possibilities, count the number of times each node had the highest stress range. Eventually, only a select number of nodes would be reoccurring.

The results from this procedure can be visualised using a probability map. For the TP this lists all the reoccurring nodes on the surface of all tubeholes and highlights their probability of having the largest $\Delta\sigma_{el}^{AB}$ stress range across all of the considered SO events. An example of such a map is presented in Figure 8. As a result, the main assessment point(s) for a single tubehole would be the node(s) which had the highest probability of having the maximum stress range, as this is the most likely to initiate a crack first. Furthermore, this also provides a rationale for examining multiple assessment locations, and the priority of which points to assess would be identified according to the probability map.

Stress predictive model

The following stage in this methodology entails formulating a predictive model which is fitted based on the data extracted from the FE results. This process is summarised as follows:

1. Identifying the key input parameters which can be used as predictors to estimate the stress state. For the TP, the maximum difference between the highest and lowest steam temperatures across the tubeplate, termed the *tilt*, was found to dominate.
2. If the resulting input-output data is not well-behaved then some further data analysis might be needed (e.g. data discrimination if the data is bimodal).
3. Fitting a predictive model to the input-output data using least-squares regression, Response-Surface or possibly artificial neural networks. For a linear model fit the following expression can be fitted to a system response or dataset [12, 9]:

$$Y = X\beta + \epsilon \tag{3}$$

where Y and X are the output and input matrices respectively. If the dataset is of size n, then Y and X are sized $n \times 1$ and $n \times p$, where p is the number of fitted parameters (e.g. $p = 2$ if a first order fit is used). β is the vector of fitted parameters (sized $p \times 1$) and ϵ is vector of residual terms (sized $n \times 1$). An estimate for β can be found using:

$$\hat{\beta} = (X^T W X)^{-1} X^T W Y \tag{4}$$

where W is an $n \times n$ diagonal matrix of weights. In the balanced case, all diagonal elements in W are equal to 1. A discussion on setting the weights can be found in [13, 14]. As a result, for predicting stresses at a specific assessment location as functions of input(s) the following expression can be used:

$$(\sigma_i) = (\mu_i) + (\epsilon_i) \tag{5}$$

where σ_i is the i^{th} stress component ($i = 1 : 6$) for a single assessment location, μ_i is the predicted mean value (obtained from $X\hat{\beta}$) and ϵ_i is the residual (error) component which is sampled from an associated histogram.

4. Investigating correlations between the stress component residuals.
5. For a wide rang of SO operating conditions, validating the probabilistic predictions given by the surrogate model against the deterministic FE data using some appropriate measure (e.g. σ_B or $\Delta\sigma_{AB}$)

For the TP, the above listed steps are discussed in detail in preliminary work reported in [5].

Correlations between stress components

Correlations between components must be considered as they have been proven to affect the quality of the probabilistic stress predictions. Even for correlations of modest strength, their effect can be important especially when there exists multiple dominant stress components, and the residual terms are large [5]. The required correlations can be interpreted as correlations between residuals (or errors) relative to the regression fit, rather than correlations between deterministically evaluated stress components. The latter correlation is indeed important, as dominant stress components are typically correlated for a range of inputs. However, that correlation is accounted for by virtue of the regression fits i.e. the six components are linked (or correlated) since they are all functions of input parameter(s). The residuals (which are treated as being independent of the input) need to be correlated separately, and are advised not to be sampled independently. Therefore, a correlations matrix (linking the residuals of the stress components) can be calculated for each assessment location.

A physical explanation as to why stresses can be significantly correlated lies in the location of the assessment point. If the assessment point lies on a free surface or an edge, which is most commonly the case, then the stress state is biaxial or uniaxial. In which case the six stress components discussed in

this work are just rotations of a biaxial or uniaxial principal stress state. For example, for a simple 2 dimensional case, the effect of rotating the stress axis from an underlying uniaxial stress state is represented by:

$$\begin{bmatrix} \sigma_{11'} \\ \sigma_{22'} \\ \sigma_{12'} \end{bmatrix} = \begin{bmatrix} c^2 & s^2 & 2sc \\ s^2 & c^2 & -2sc \\ -sc & sc & c^2 - s^2 \end{bmatrix} \begin{bmatrix} \sigma_{11} \\ 0 \\ 0 \end{bmatrix} \tag{6}$$

where c and s are the *cosine* an *sine* of the rotational angle. Therefore, these correlations are, at least in part, attributed to fixing the orientation of the stress axis for the entire FE model. This makes conducting the R5 V2/3 more straightforward because the orientation of each stress component is kept fixed. When this procedure is conducted for a fixed location, then what is of interest is the change in one stress component from one SO event to the next. Therefore, these correlations essentially represent the relative orientation of the global axis with respect to the local principal axis. As a result, these correlations are location specific and must be inferred from stress results taken from the same node in the FE model.

Metal temperature modelling

Predicting the MT was based on the observation that it would be strongly linked to the input steam temperatures. Thus the proposed approach for predicting the MT for a specific assessment location for a specific event uses the following expression:

$$T_M = T_S + \Delta T \tag{7}$$

T_M is the metal temperature and T_S is the stream temperature. The latter is taken as a deterministic input which is given by the processed history data, while ΔT is sampled from an appropriate histogram (for an example see Figure 11).

3. CASE-STUDY: THE TUBEPLATE (TP) PLANT COMPONENT

3.1. COMPONENT DESCRIPTION

The TP is a cylindrical component which has 37 tubeholes and is made of type 316H stainless steel forging. The failure mechanisms are driven by creep-fatigue, large thermal transients and over-heating due to tube restrictions. Due to legacy work that has been done on this component, two separate FE geometries have been used: a sixth model (Figure 1a) for transient events and a full model (Figure 1b) for steady-operation events. Figure 2 shows the location of the start-of-dwell stress (σ_B, point B) at an intermediate position in the hysteresis cycle, which is typical for a point near the surface of a tube bore. During a start-up (SU) transient, the surface of a tubehole is heated up while the surrounding metal remains colder, thus the difference in thermal expansion produces a compressive stress (point A in Figure 2) near the surface of the tubehole. The reverse effect occurs during a reactor-trip (RT) transient where a tensile stress (point C) is induced on the surface. Point B can include periods during which large temperature gradients are induced by boiler instabilities which in turn lead to large thermal stresses.

3.2. Transient loading results

Figures 5 show examples of the processed transient FE data for a single assessment location. Across the events examined, the SU and RT events which had the most severe stress states at an assessment location of interest are summarised in Table 1. In addition to stresses, metal temperature data was also extracted from the FE results. Metal temperatures are important in creep-fatigue assessments as they may influence the material properties used for characterising the cycle extremities and creep rates. Figure 6 shows histograms of metal temperature data based on the all the available SU and RT events.

For each of the two considered transient types (SU and RT) correlations matrices linking the six SCs where constructed . For the SU events, which in

Table 1: Most severe transients out of the examined SU and RT events for single assessment location of interest.

	Stress components [MPa]						**Metal temp.** $[^{\circ}C]$
	σ_{11}	σ_{22}	σ_{33}	σ_{12}	σ_{13}	σ_{23}	
SU	12.58	-271.60	5.68	0.08	-0.11	-1.04	439.6
RT	-4.99	196.70	-4.16	-0.03	0.05	0.80	372.8

some cases had very strong (> 0.9) correlation coefficients, is:

$$\begin{bmatrix} 1.00 & 0.96 & 0.99 & -0.72 & 0.46 & -0.50 \\ 0.96 & 1.00 & 0.97 & -0.65 & 0.31 & -0.46 \\ 0.99 & 0.97 & 1.00 & -0.71 & 0.44 & -0.50 \\ -0.72 & -0.65 & -0.71 & 1.00 & -0.27 & 0.87 \\ 0.46 & 0.31 & 0.44 & -0.27 & 1.00 & 0.06 \\ -0.50 & -0.46 & -0.50 & 0.88 & 0.06 & 1.00 \end{bmatrix} \tag{8}$$

This correlation matrix relates to the six stress components according to this order: σ_{11}, σ_{22}, σ_{33}, σ_{12}, σ_{13} and σ_{23}. It worth highlighting that due to the approach taken for extracting stresses from the FE models, namely focusing on surface nodes, the stress states are likely to be biaxial or uniaxial if stresses are taken from an element located on a free surface or an edge. Therefore, the correlations between stress components are likely due to the reorientation of stresses relative to the local principal axis.

For SU and RT, Figure 7 shows histograms of the Spearman correlation between metal temperatures and the most dominant stress component. For both transient types, often a strong negative correlation was observed. To clarify, for SU the stresses were kept compressive (i.e. negative) when calculating these corrections. Therefore, the correlations in Figure 7a indicate that a low temperature correlates with a smaller compressive stress. A physical explanation for these correlations is that the point that has a high temperature relative to it's

surroundings will try to expand but will experience a compressive stress due to the constraint from the colder surrounding points, which is the case for a SU transient. For RT the reverse is correct; the point in question tries to contract but is stretched by its hotter surrounding points, therefore producing a high tensile stress.

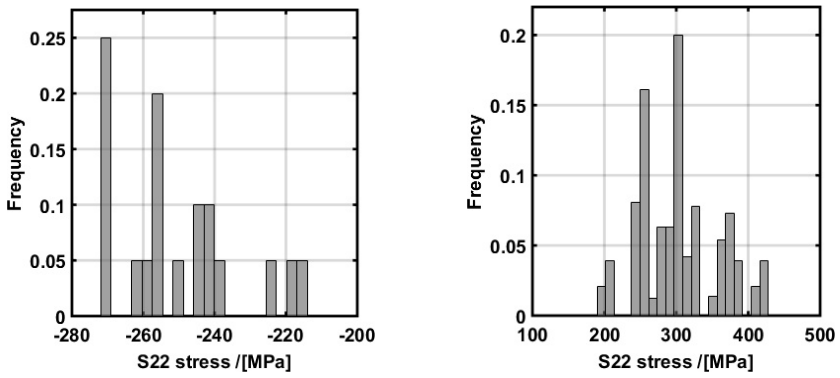

(a) SU (b) RT

Figure 5: For Tubehole 2 ($TN = 2$) and for the examined SU and RT transient events (20 and 18 events respectively), this figure shows histograms of the processed FE data for direct stress components. For each plot, the sum of frequencies is equal to one.

3.3. Steady-operation loading results

The methodology for SO loading was applied to the TP as its historic data was processed and 1300+ steady-operation events were run in FE to produce metal temperature and stress results. Thereafter, the main assessment locations (nodes) for each tubehole where identified by finding the locations which most frequently produced the largest $\Delta\sigma_{el}^{AB}$ across the 1300+ FE runs. The outcome was the probability map shown in Figure 8, which shows that only a select number of surface nodes would be expected to frequently have the largest stress ranges. For example, for Tubehole 2 ($T = 2$), one node had 50% chance to have the largest stress range. This map provided a rationale to select a limited number of nodes per tubehole on which to focus assessment efforts, as these are

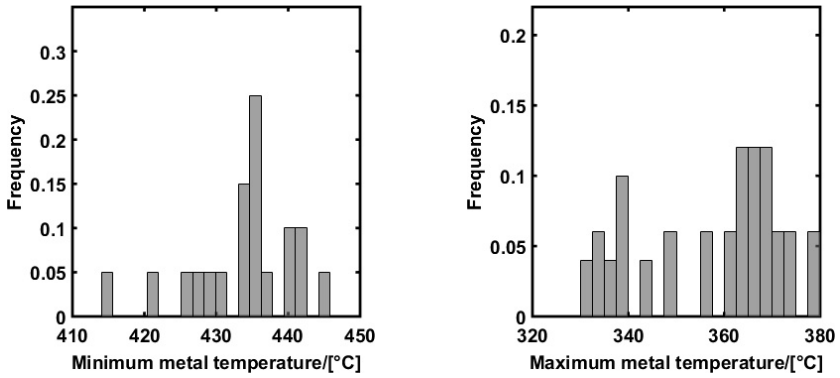

(a) SU (b) RT

Figure 6: Histograms of metal temperatures (the temperatures used for the assessment) based on data for Tube 2 across all 20 SU and 18 RT events. Medians were $435.60°C$and $362.76°C$ for SU and RT events respectively. For each plot, the sum of frequencies is equal to one.

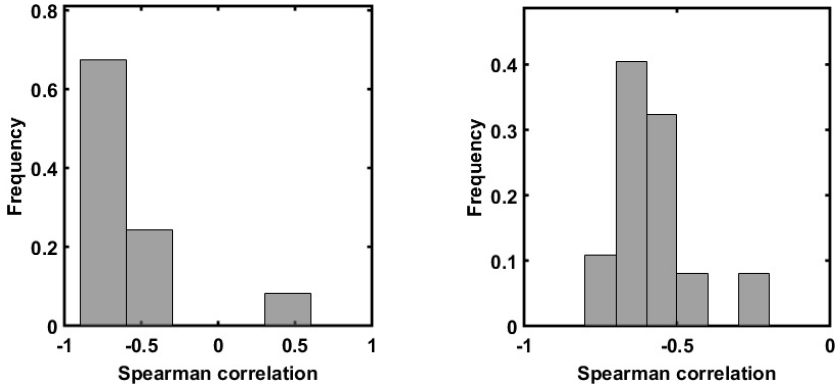

(a) SU (b) RT

Figure 7: Across all 37 tubes, histograms of Spearman correlations coefficients between the assessment metal temperature (see Figure 6) and the most dominant stress component (σ_{22}) for SU (see Figure 5a) and RT (see Figure 5b). For each plot, the sum of frequencies is equal to one.

the most likely to initiate a crack.

The following stage was to extract the FE results from the chosen assessment locations. The output of interest were the six SCs and the metal temperatures

at the assessment locations. It was required to identify the key inputs which are later used to infer stresses. Various input parameters were postulated and trialed [5], but only one seemed to strongly dominate all 6 SCs, which was the tilt. The latter is defined as the steam temperature difference between the hottest and coldest tubeholes. The conclusion was that the tilt strongly dominated the output stress state, and thus only this input parameter was deemed to be worth considering at this stage.

The relationship between each SC and tilt exhibited a multi-modal behaviour, as shown in Figures 9. A possible explanation for this behaviour might be the existence of another input parameter which was not identified i.e. the plot in Figure 9 only shows a slice of a multidimensional surface. However, no such parameter was successfully identified for the TP. For the purposes of the application at hand, it was deemed appropriate to segregate each stress component dataset into three distinct modes. A discussion on the use of discrimination using *Bayesian discriminant rule* can be found in [15] and, based on the same principles, [16] provides various data analysis tools in MATLAB®, which includes the *rda* function which was implemented to segregate the processed FE data into three modes . For reference, these results were for Tubehole 2 ($T = 2$) taken at the nodal location that had 50% chance of having the largest stress range (see Figure 8). The modes across all stress components do (almost) perfectly correlate. That means if one point is part of Mode 1 for one stress component, it will (almost always) lie on the same mode for the other 5 components.

After segregating the input-output datasets (6 sets, one per SC), least-squares regression was used to fit linear models to the data. Figure 9 shows datasets for the most dominant SC as functions of input tilt, segregated into 3 modes and with the appropriate least-squares fits. It was judged that Mode 3 subsets can be disaggregated, and this was believed to be conservative. The Mode 3 was consistently compressive and therefore would not increase creep damage (within the context of R5 in any case). As a result, these subsets were

disaggregated for simplicity as this is judged to be conservative. Therefore, only Modes 1 and 2 were considered in the proposed predictive model for the TP. Figures 9 also shows the residuals relative to the regression fits presented as histograms. Theses histograms were used to model the statistical model uncertainty (ϵ_i in Equation 5)) for each stress component.

A Monte-Carlo simulation (MCS) was implemented to produce probabilistic stress range predictions for the full range of possible input tilts, the outcome of which is shown in Figure 10. The inputs for this MCS were the stochastically modelled stress components using Equation 5, where the mean stress was obtained from the least-squares fit and the error term was produced by sampling the histograms shown in Figure 9. Correlations between stress component residuals (see Equation 9) were also incorporated and were found to significantly affect the sought probabilistic $\Delta\sigma_{el}^{AB}$ predictions. Figure 10 also shows the $\Delta\sigma_{el}^{AB}$ calculated from the original processed FE results (the deterministic data used to construct the predictive model). This data was superimposed on the $\Delta\sigma_{el}^{AB}$ predictions for verification purposes. The predictions were consistent with the deterministic data, and only a small number of data points lies outside the envelope (maximum-minimum and upper-lower confidence limits in Figure 10) produced by the probabilistic predictions. This was believed to be acceptable because the predictions were consistently higher than the points outside the envelope, and therefore was considered conservative.

Figure 11 shows a histogram of the differences between the metal and steam temperatures for all of the 1300+ SO events which were considered. These results suggest that an underlying distribution does exist, and can be sampled to stochastically model the random variable ΔT in Equation 7. With temperatures being as important as stresses for promoting creep damage, it was judged that correlations between ΔT and the stress component residuals should also be incorporated for their importance in a prospective probabilistic assessment. A 7×7 matrix which links not only stress component residuals, but also links

these residuals and ΔT was computed. For the same assessment location as the one considered in Figure 9, the correlations matrix was as follows:

$$\left[\begin{array}{cccccc|c} 1.00 & 0.05 & 0.04 & 0.52 & 0.05 & 0.09 & -0.02 \\ 0.05 & 1.00 & 0.62 & 0.35 & 0.62 & 0.71 & 0.70 \\ 0.04 & 0.62 & 1.00 & 0.58 & 1.00 & 0.52 & 0.57 \\ 0.52 & 0.35 & 0.58 & 1.00 & 0.59 & 0.30 & 0.18 \\ 0.05 & 0.62 & 1.00 & 0.59 & 1.00 & 0.52 & 0.56 \\ 0.09 & 0.71 & 0.52 & 0.30 & 0.52 & 1.00 & 0.88 \\ \hline -0.02 & 0.70 & 0.57 & 0.18 & 0.56 & 0.88 & 1.00 \end{array}\right] \quad (9)$$

with the bottom and far right elements of this matrix relating ΔT with the stress component residuals.

4. FURTHER CONSIDERATIONS FOR PROBABILISTIC IMPLEMENTATION

4.1. Sampling

Consider a component history that is divided into discrete cycles with each having peak transient stresses during the start and end of the cycle. The peak transient stresses for SU and RT events are denoted by points A and C respectively in Figure 2. When conducting a probabilistic assessment of a component (e.g. using a MCS with N trials), each cycle transient can have N possible stress states and metal temperatures. This requires a sampling strategy in order to ultimately translate the available plant data for the transient events of interest into the samples required for a MCS. Given a transient type, it is deemed appropriate to assume that the samples assigned to different cycles should be treated as uncorrelated. This effectively means that there is no reason to believe that the transient for one cycle is affected by the same transient type from the subsequent or preceding cycle(s). Therefore, each transient within a given history is treated independently of: transients of the same type but from other cycles, and transient of other types from any cycle.

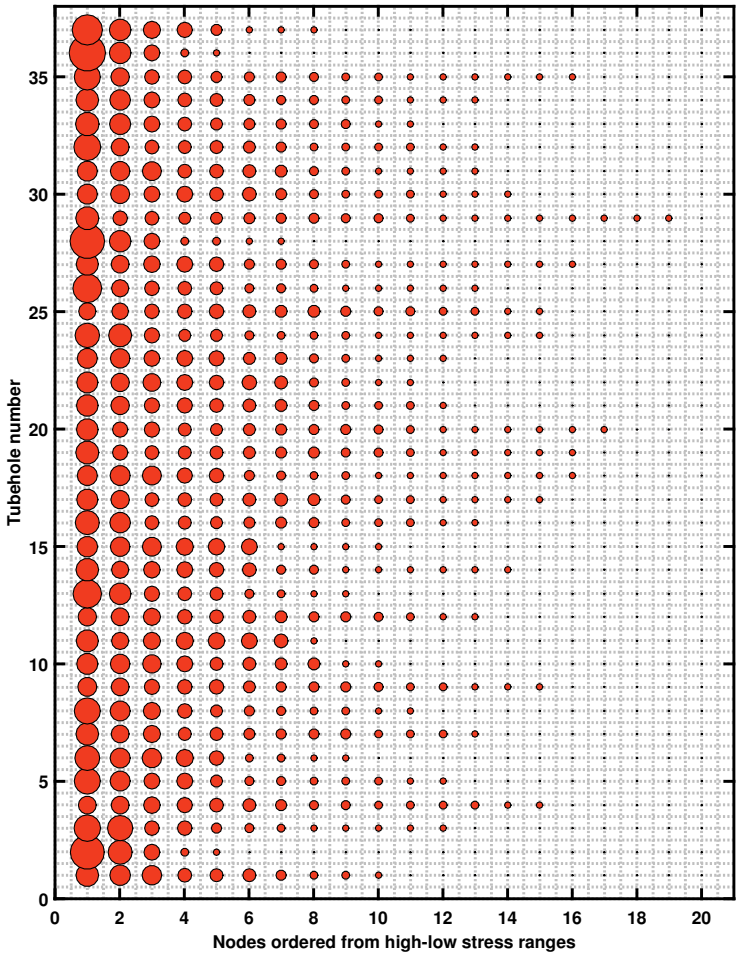

Figure 8: A probability map showing the relative frequency of 20 nodes on each tubehole ($1-20$ on the horizontal axis) having the largest stress range, for all tubes ($T = 1-37$ on the vertical axis). The size of each point is a measure of probability.

For a single cycle, there are two proposed approaches which can be adopted for incorporating assessment metal temperatures (Figure 6) and stresses (Figures 5 in a prospective probabilistic assessment for a desired number of N trials. For a given transient type these are:

1. Sampling metal temperature and stress components from tubehole specific histograms independently and then introduce correlations at a later

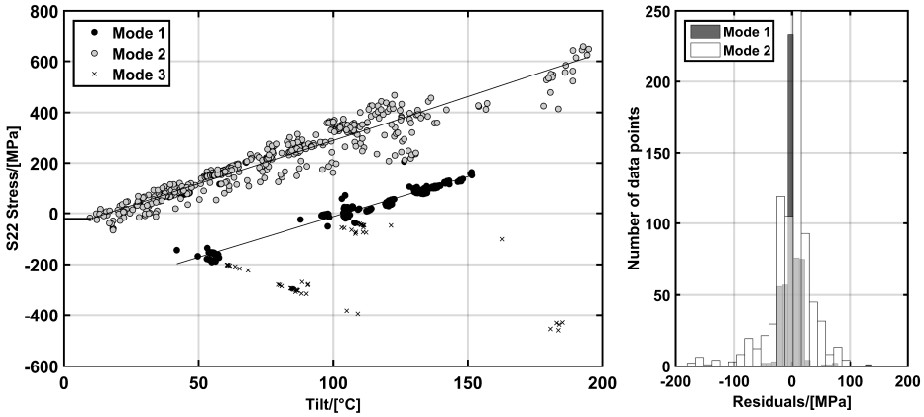

Figure 9: The processed FE data corresponding to the dominant stress component (σ_{22}) segregated into three distinct subsets. These results are specific to tubehole 2, at the location most probable to have the largest stress range (see Figure 8).

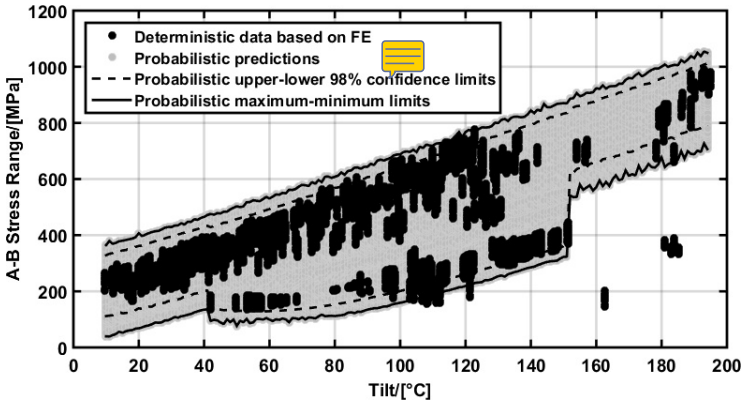

Figure 10: For tubehole 2 (i.e. T = 2) at the location most probable to crack initiate, this figure shows probabilistic stress predictions for a range of tilts superimposed onto the deterministic values of $\Delta\sigma_{el}^{AB}$ for verification purposes.

370 stage. This requires quantifying the relevant correlations and exercising judgement as to which correlations to be included.

2. A *bootstrapping* approach which simply considers how may transient events are available (N_{TE}, e.g. 20 SU events in the case-study) and then assigns $1/N_{TE}$ of the N samples the metal temperature and stress state associ-

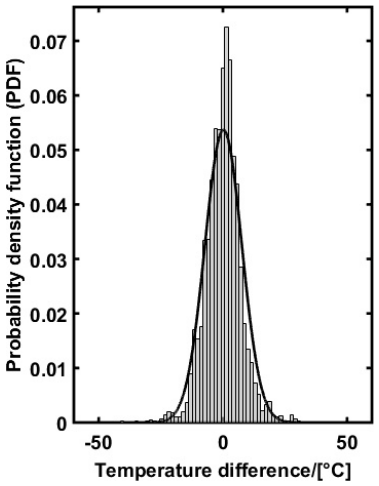

Figure 11: Histogram of the differences between steam and metal temperatures (ΔT) for all tubeholes across 1300+ events modelled using the thermal FE model. A fitted normal distribution is also shown superimposed on the data.

ated with one of the N_{TE} transient events. If this sampling strategy is adopted, then correlations need not be considered because each sample would be taken from a pool of coupled SCs and MT data. This effectively means that correlations would be accounted for at the sampling stage.

The former approach is deemed more appropriate if a large number of transient events is available which provides an opportunity for rigorous statistical characterisation. The latter approach, is more suited for situations where a limited number of events is considered, and is more appropriate for the examined case-study. For a prospective probabilistic assessment, the rationalisation given in this section ensures that every transient during the entire history of the component will be assigned every possible transient condition according to the available plant data.

For steady-operation, a component history consists of cycles which in turn are divided into discrete events. Based on the predictive models discussed in this paper, for each event 6 $\times$ SCs and 1 $\times$ MT (and their respective uncer-

tainties) can be obtained. For predicting the MT of an assessment location for a single event (using Equation 7), T_S can be read directly from the processed history data, and the uncertainty ΔT can be sampled once from an appropriate histogram.

4.2. Stress and temperature permutations

One of the very initial stages of setting up a Monte-Carlo simulation (MCS) is the sampling of the uncertain input parameters according to their probability distributions, with the number of samples being equal to the number of desired trials, N. What follows is the arranging of the sampled input parameters to form the input sets for each of the MCS trials; for a single trial all input parameters are set to fixed values. After sampling, *random permutations* can be produced to rearrange all sampled inputs, with the number of permutations required being equal to the number of input parameters. This concept forms a key feature of the LHS approach, which ensures that each sample (or *bin*) of each input will be used exactly once, though not all possible combinations of all input parameters can be trialed of course [17].

Setting these permutations can require some judgement, a topic which is discussed in [17]. For a time *independent* material property, for example, a permutation is formed as part of a Latin-hypercube at the start of the probabilistic code, and this remains unchanged for the whole simulation. The same concept is not applicable to time dependent input parameters such as thermal stresses and metal temperatures, which are in fact ever changing during the lifetime of the component. Given the discretisation of the loading history into events, each event is required to experience all possible stress and temperature samples over the course of the MCS. Therefore, ideally a set of permutations is required per event within the loading history. In a deterministic sense, a change from one event to the next warrants a change in metal temperatures and stresses. When considering how often the loading permutations need to be reproduced (e.g. whether at each event or cycle) judgement needs to be exercised. Nevertheless,

there are commonly three possible options:

1. Using a fixed loading permutation for the entire history (as if stresses and temperatures were material properties). This implies that the loading for all cycles and all events are perfectly correlated, which is erroneous. So this option is easily discarded.
2. The loading permutation is reproduced at each event in time.
3. Each cycle will have its own independent permutation.

The first option is the most conservative of the three, and it is not physically justifiable. Therefore, this option is advised to never be used. The second and third options are closer to a physical situation, however, from one cycle to the next the distribution of temperatures over the tubeplate can change substantially, and as such using a new permutation at each cycle is not unrealistic. Therefore, the latter option is considered the most ideal, but it still is not physically perfect. As to which of the second and third options is more conservative it depends on the component application of interest, its loading history and the construction of the probabilistic assessment.

4.3. Incorporating material property uncertainties

The FE models used in this work are purely elastic models. In terms of material properties required as inputs to the FE models, Young's modulus (E) and the coefficient of thermal expansion (α) are the two key quantities. Given that in a probabilistic assessment these properties can be treated as uncertain variables, their scatter can affect the results of the FE models used. The scatter in E and α both independently result in a proportional variability in any strain controlled stresses, for example thermal stresses, whilst primary stresses should remain unaffected. Therefore, a scaling factors, U_E and U_α, can be defined according to the variabilities of E and α relative to their mean values (μ_E and μ_α, which are the fixed value used in the FE models). For instance, the scaling factor for E would be defined as:

$$U_E = \frac{E}{\mu_E} \tag{10}$$

where E is treated stochastically. In a probabilistic assessment, U_E is essentially a proxy for E, and therefore, must not be sampled independently from the latter. These scaling factors can be quite significant. For example, if the 95% upper and lower bounds are considered to be $1.6445 \times \sigma_E$ away from the mean, where σ_E is the standard deviation, then U_E can range between 0.89 and 1.11. The stress results presented in the case-study include contributions from both mechanical (primary) and thermal (secondary) loads. So applying these factors to the stress results is not strictly correct, as only thermal stresses should be factored. Nevertheless, an exception can be made in situations where primary stresses are significantly smaller than thermal stresses, which is the case for the TP. Therefore, an assumption can be made that such error is not significant and the approach discussed above can be adopted for its simplicity, and is believed to be slightly conservative. Consequently, two independent factors (assuming E and α are not correlated) can be applied to the stress results to account for the variabilities of material properties they respectively represent.

5. CONCLUDING REMARKS

With the increase in popularity of using probabilistic techniques in creep-fatigue assessments, there is a need for systematic approaches for examining uncertainties in loading conditions that are informed by plant measurements. In this work, a number of techniques have been explored and two possible approaches were suggested for dealing with two loading event types (transient, TR, and steady-operation, SO) separately. A tubeplate component was used as part of a case-study to demonstrate the utilities of the suggested approaches. The main reason for using different methods for characterising the two event types was that TR events usually occur far less frequently than SO events and therefore less data is available for examining their variability.

For TR events it was considered appropriate to treat the historical events (for which data is available) as constituting the range of possibilities for each

transient event occurring within the lifetime of the component. Therefore, the proposed approach was based on examining numerous transient events to characterise the variability of transient input parameters (stresses and temperatures) in creep-fatigue assessments. What follows is processing the plant data, running the events in FE models, and extracting the desired characteristic TR quantities. Histograms can be constructed to examine the variability of each stress component for each of the assessment locations. Correlations must also be examined for transients, with the main conclusion that two types are of importance for a single assessment location: correlations between SCs, and the correlations between each SC and the MT. The final stage was to sample the processed transient data in preparation for use in a probabilistic assessment of the plant component. Cycles within a component loading history are considered independent of each other. Sampling for a single cycle is conducted such that every transient within any cycle during the entire history of the component will be assigned a range of possible transient conditions dictated by the available plant data.

For SO events, surrogate models where constructed which allowed the prediction of stresses and metal temperatures with associated uncertainty based on some key input parameter(s). The approach for SO events was only possible due to the abundance of relevant historic data. Firstly, the raw plant data required processing in order to discretise the entire historic data into SO events. Then a batch of these events, covering a wide range of possible operating situations was run in FE models to obtain the characteristic SCs and MT for each of these events. The FE results were then processed in order to: establish the locations in the FE model space which are most likely to crack, and then extract the SCs and MT data from these locations. The outcome of the latter stage was termed the *processed FE data*. Thereafter, a simple sensitivity study can be conducted to identify the key input parameters which could be used to predict the desired SCs using a statistical model (e.g. linear regression). Furthermore, correlations between stresses and metal temperatures should also be investigated and

included. Finally a verification stage was added to inspect the stress range results based on the predictive probabilistic model to ensure the predictions are representative of the original processed FE stresses. To demonstrate the above summarised approach, an example examining the TP for treating steady-state stresses during nominal plant operation was presented.

Finally, part of this paper was devoted to discussing importation considerations for the implementation of the results obtained from the above proposed approaches in probabilstic CF damage assessments. The value of these approaches lies in providing a means for incorporating loading uncertainty, thus reducing conservatism and making better utilisation of the available plant data. Additionally, especially for SO events, the proposed approach avoids resorting to running time consuming FE models multiple times within one probabilistic MCS, which would be computationally prohibitive.

ACKNOWLEDGMENTS

The authors would like to express their gratitude for the support of EDF Energy towards this project and in particular Marc Chevalier and Joy Tao.

6. REFERENCES

[1] EDF Energy Nuclear Generation Ltd, R5 Issue 3 Volume 2/3 (Rev.002): Creep-Fatigue Crack Initiation Procedure for Defect-Free Structures. Assessment Procedure for the High Temperature Response of Structures (Nov, 2014).

[2] D. W. Dean, P. J. Budden, R. A. Ainsworth, R5 Procedures for Assessing the High Temperature Response of Structures: Current Status and Future Developments. Proceedings of ASME PVP2007, July 22-26, 2007, San Antonio, Texas, USA, paper PVP2007-26569.

[3] N. A. Zentuti, J. D. Booker, R. A. W. Bradford, C. E. Truman, A review of probabilistic techniques: towards developing a probabilistic lifetime methodology in the creep regime, Materials at High Temperatures 34 (5-6) (2017) 333–341.

[4] Y. M. Goh, The Incorporation of Uncertainty into Engineering Knowledge Managment, Ph.D. thesis, University of Bristol (2005 Jan).

[5] N. A. Zentuti, J. D. Booker, R. A. W. Bradford, C. E. Truman, Management of complex loading histories for use in probabilistic creep-fatigue damage assessments, Proceedings of the ASME 2018 Pressure Vessels & Piping Conference. Codes and Standards, PVP2018-84400, July, 2018.

[6] N. A. Zentuti, J. D. Booker, R. A. W. Bradford, C. E. Truman, Correlations between creep parameters and application to probabilistic damage assessments, International Journal of Pressure Vessels and Piping 165 (2018) 295 – 305.

[7] Matworks, Generate Correlated Data Using Rank Correlation, `https://uk.mathworks.com/help/stats/generate-correlated-data-using-rank-correlation.html`, accessed May 30, 2017 (2017).

[8] M. C. Cario, B. L. Nelson, Modelling and generating random vectors with arbitrary marginal distributions and correlation matrix, Tech. rep., Delphi Packard Electric Systems (Warren, OH) and Department of Industrial Engineering and Management Science, Northwestern University (Evanston, IL) (1997).

[9] J. Wallace, R. Wang, D. Mavris, Creep Life Uncertainty Assessment of a Gas Turbine Airfoil, 44th AIAA/ASME/ASCE/AHS/ASC Structures, Structural Dynamics, and Materials Conference. American Institute of Aeronautics and Astronautics, Apr, 2003.

[10] Z. Liu, D. Mavris, A Methodology for Probabilistic Creep-Fatigue Life Assessment of Hot Gas Path Components, 45th AIAA/ASME/ASCE/AHS/ASC Structures, Structural Dynamics & Materials Conference. American Institute of Aeronautics and Astronautics, Apr, 2004.

[11] Y. M. Goh, J. Booker, C. McMahon, A Comparison of Methods in Probabilistic Design Based on Computational and Modelling Issues, Springer Netherlands, Dordrecht, 2005, pp. 109–122.

[12] M. A. Bezerra, R. E. Santelli, E. P. Oliveira, L. S. Villar, L. A. Escaleira, Response surface methodology (rsm) as a tool for optimization in analytical chemistry, Talanta 76 (5) (2008) 965 – 977.

[13] L. Gutkin, S. Datla, C. Manu, Pilot study for uncertainty analysis in probabilistic fitness-for-service evaluations of zr-2.5nb pressure tubes: Uncertainty characterization, Proceedings of the ASME 2018 Pressure Vessels & Piping Conference. Codes and Standards, PVP2018-85011, July, 2018.

[14] M. Kutner, C. Nachtsheim, J. Neterand, W. Li, Applied Linear Statistical Models, 5th Edition, The McGraw-Hill/Irwin series operations and decision sciences, McGraw-Hill Irwin, London, 2005.

[15] M. Hubert, K. V. Driessen, Fast and robust discriminant analysis, Computational Statistics and Data Analysis 45 (2) (2004) 301 – 320.

[16] S. Verboven, M. Hubert, Libra: a matlab library for robust analysis, Chemometrics and Intelligent Laboratory Systems 75 (2) (2005) 127 – 136.

[17] R. A. W. Bradford, A Procedure for Probabilistic Creep-Fatigue Crack Initiation Assessment Consistent With R5 Volume 2/3, Tech. Rep. E/REP/BBAB/0028/GEN/13, EDF Energy Nuclear Generation Limited (Jan. 2014).